Contents lists available at ScienceDirect

Journal of Physics and Chemistry of Solids
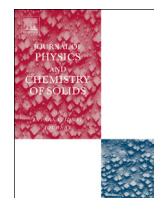
Spectroscopic properties of Nd^{3+}-doped tungsten–tellurite glasses

F.B. Costa [a], K. Yukimitu [a], L.A.O. Nunes [b], M.S. Figueiredo [c], L.H.C. Andrade [d], S.M. Lima [d], J.C.S. Moraes [a,*]

[a] *Faculdade de Engenharia, UNESP – Univ Estadual Paulista, Campus de Ilha Solteira, SP, Brazil*
[b] *Laboratório de Laser e Aplicações, IFSC, São Carlos, SP, Brazil*
[c] *UFGD, Dourados, MS, Brazil*
[d] *Grupo de Espectroscopia Óptica e Fototérmica, UEMS, Dourados, MS, Brazil*

ARTICLE INFO

ABSTRACT

In this work, we investigate the spectroscopy properties of neodymium doped tungsten–tellurite glasses prepared in ambient and O_2-rich atmospheres. A conversion of TeO_4 to TeO_3 units was caused by the addition of Nd^{3+} into the glass, which was confirmed by absorption spectra and by Judd–Ofelt parameter behavior. The relaxation of the $^4F_{3/2}$ level is dominated by radiative decay and cross-relaxation between Nd^{3+} and Nd^{3+} ions. The energy transfer from Nd^{3+} to the hydroxyl group is negligible when compared to the cross-relaxation. The luminescence quantum efficiency values of the $^4F_{3/2}$ level decreases as the Nd^{3+} concentration increases, independently if determined by the Judd–Ofelt method or by the thermal lens technique. The observed reduction in the IR absorption associated to OH groups was not effective to improve the luminescence quantum efficiency.

1. Introduction

Several rare earth (RE) ions have been studied for laser application. Among them, the Nd^{3+} ion is one of the most investigated, mainly due its large cross-sections of optical absorption near 800 nm ($^4I_{9/2} \rightarrow {}^2H_{9/2} + {}^4F_{5/2}$), which turn easiest the excitation by diode laser, and the high quantum efficiency of the $^4F_{3/2} \rightarrow {}^4I_{11/2}$ emission near 1060 nm. Moreover, as the $^4I_{11/2}$ energy level is ~ 2000 cm^{-1} above the ground state, this turn the system as four level one, which it is well known to favor the population inversion avoiding the re-absorption effect. Lasing has been obtained in different bulk glasses doped with Nd^{3+} ions [1–7], but the tellurite-based glasses have attracted special interest since Wang et al. were able to fabricate active tellurite glass fiber laser [1]. Tellurite glasses combine the attributes of reasonable thermal stability, high refractive index, high solubility of RE ions (some tellurite glasses may dissolve up to 25% of RE oxides [8]), larger absorption and emission cross-sections, and low phonon energy compared to the silicate, phosphate, and borate glasses [8,9], with a wide transmission window in the infrared region [9].

In particular, the RE doped tungsten–tellurite glasses have been shown to have excellent properties for applications such as planar waveguides [10,11], amplifiers [12], lasers [4,5], single mode fiber lasers [13,14], and second harmonic generation devices [15]. However, tungsten–tellurite glasses have larger amounts of water when melted in air. The water is incorporated into the glass as hydroxyl (OH) groups, which have a strong and broad vibrational absorption band of between 2000 and 3600 cm^{-1}, promoting the energy loss. The absorption losses due to OH groups are disadvantageous because they decrease the electronic population of the $^4F_{3/2}$ excited level. This decreases luminescence quantum efficiency (η), hindering the practical use of these glasses [16–18]. Zhang and Hu [19] studied the influence of the OH$^-$ content on IR emission of Nd^{3+}, Yb^{3+}, and Er^{3+}-doped tetraphosphate glasses. They observed that OH$^-$ has a large effect on the IR emission of these RE ions and that the IR luminescence decay rate increases linearly with OH$^-$ concentration. Wang et al. [17] observed that, by reducing the OH$^-$ content in Yb^{3+}-doped tellurite glasses, the lifetime luminescence increased from 0.7 to 1.22 ms, indicating an improvement of the optical gain.

In this paper, we investigate the behavior of the spectroscopic properties of the Nd^{3+}-doped tungsten–tellurite glasses in function of the neodymium concentration with samples prepared in ambient and oxygen-rich atmospheres. Luminescence quantum efficiency was determined by applying the thermal lens (TL) technique in the samples, and the obtained results were confronted with those determined by the relationship between experimental luminescence lifetime and radiative lifetime calculated

* Correspondence to: Departamento de Física e Química – UNESP, Campus de Ilha Solteira, Av. Brasil 56, 15385-000 Ilha Solteira, SP, Brazil.
E-mail address: joca@dfq.feis.unesp.br (J.C.S. Moraes).

by the Judd–Ofelt (JO) theory.

2. Experimental

Two sets of tungsten–tellurite glass samples with nominal composition $(100-x)(0.8TeO_2+0.2WO_3)+x\text{Nd}_2\text{O}_3$, where $x=0$, 0.05, 0.5, 1, 2, and 4 mol%, were prepared by conventional melt-quenching method in ambient (Amb) or O_2-rich (O_2) atmospheres. Table. 1 shows the nominal composition (mol%) of the glasses. For the set prepared in the Amb atmosphere, grade reagents of the Sigma-Aldrich (with $>99\%$ or higher purity) were weighted, mixed into an agate mortar, and melted in a platinum crucible at 880 °C for 30 min. The melt was poured into a stainless-steel mold pre-heated near the glass transition temperature ($T_g \sim 350$ °C). For the set prepared in an O_2 atmosphere, the furnace was placed inside a sealed chamber, where a vacuum was created. This was followed by an injection of O_2 (until the inner pressure reached 1 atm), and the same procedures were carried out. After their contents were poured, the glasses were returned to the other furnace for annealing in order to reduce mechanical stress. The annealing occurred for 2 h at T_g temperature, and then the sample was slowly cooled to room temperature. Finally, the produced glasses were cut and polished, reaching thicknesses of between 0.71 and 0.95 mm.

All of the samples exhibited good optical quality, without any scattering point or bubble, and the glassy state in these samples was confirmed by X-ray diffraction (XRD) analysis using Cu K$_\alpha$ radiation. The densities (Table 1) of the samples were determined by Archimedes' method, using distilled water as the immersion liquid.

Fourier transform infrared (FTIR) spectroscopy was performed using a Nicolet Nexus 670 FTIR spectrometer. The absorption spectra of the bulk samples were recorded in the range of 2000–4000 cm^{-1} using 64 scans, a resolution of 4 cm^{-1}, and a N$_2$ purge. Raman measurements were carried out by exciting the samples under 514.5 nm with an Ar+ laser (Innova 308C model, Coherent). Confocal lenses with 4 mm of focal length were used to focus the laser beam into the samples, and to detect the Raman signal. The scattering light was filtered by an edge filter and it was focused in an optical fiber coupled in a monochromator (iHR 320 model, Horiba Jobin Yvon) with CCD (Sygnature Hamamatsu S3903-1024Q PDA) for detection. The ground state absorption spectra of the glasses were obtained by using a Perkin Elmer Lambda 900 UV/VIS/NIR spectrophotometer in the range of 400–925 nm.

The luminescence $^4F_{3/2} \rightarrow {}^4I_J$ ($J=13/2$, 11/2 and 9/2) was measured by excitation at 514.5 nm with an argon laser and corrected by Nd^{3+} nominal concentration values to ensure that all samples absorbed the same amount of photons. The luminescence lifetime measurements of the $^4F_{3/2}$ level were obtained using 808 nm wavelength radiation generated by an optical parametric oscillator (OPO) pumped by a 5 ns pulsed Nd:YAG laser (355 nm, 10 Hz).

The TL technique was used to measure the fraction of the absorbed energy that was converted into heat by the samples. This result could be used to calculate the luminescence quantum efficiency. The TL setup was a two beam mode-mismatched configuration that used a Ti:Sapphire laser tuned at 808 nm as the excitation source and a HeNe laser at 632.8 nm to probe the TL effect. The experimental curves were fitted using the theoretical model proposed by Shen et al. [20]. The experimental geometrical parameters were $m=8.4$ and $V=1.8$. Further details of the experimental arrangement can be found in the reference [21].

3. Results and discussion

Fig. 1 shows a comparison between spectra of the TW-1Nd glasses prepared in Amb and O_2 atmospheres. The amplitude of the absorption bands centered at 3160 and $\sim$2200 cm^{-1} were reduced on the average of 48% and 44%, respectively, when O_2 atmosphere was used to prepare the samples. These bands have been ascribed to the stretching mode of the weakly and strongly hydrogen-bonded Te–OH…O–Te groups, respectively [22,23]. This result indicates that O_2 atmosphere was efficient to reduce the OH ions content in the bulk.

Fig. 2 shows the absorption spectra of the Nd^{3+}-doped TW glasses prepared in the O_2 atmosphere in the spectral range of 400–925 nm. Each spectrum presents eight absorption bands located at 514, 527, 585, 628, 682, 748, 808, and 874 nm. The addition of Nd^{3+} caused an increase in the intensity of the absorption peaks and a blue-shift of the absorption edge. The inset of Fig. 2 shows the correlation between peak area (804 nm) and Nd^{3+} concentration for glasses prepared in the Amb and O_2 atmospheres, indicating that the incorporation of neodymium in the glass was effective. The same behavior was observed in the area of the other absorption peaks. The spectra of the samples prepared in the Amb and O_2 atmospheres were similar in this spectral region.

The blue-shift of the absorption edge has been observed in previous studies [24–26], and it has been related to the changes in the glass structural units. Nazabal et al. [25] studied the TeO$_2$–ZnO–ZnF$_2$ glass doped with erbium and attributed to the blue-shift the structural conversion from TeO$_4$ (tbp=trigonal bipyramid) towards TeO$_{3+1}$ and TeO$_3$ (tp=trigonal pyramid) units. From Raman spectra of the samples, it was observed that the introduction of Nd^{3+} ions in the glass led to a similar variation in the glass network, for the two atmospheres in which the glasses were prepared. Fig. 3a shows the Raman spectra of the TW and TW-4Nd, both prepared in O_2 atmosphere, in the 1100–500 cm^{-1} range. The spectra shown a sharp scattering band located at 930 cm^{-1} and a broad band around 700 cm^{-1}. The first band correspond to the stretching vibrations of W–O$^-$ and/or W=O in the WO$_4$ and WO$_6$ units [27,28], respectively. The observed decrease in the absorption band at 930 cm^{-1} can be due to W ion coordination states changes from sixfold [WO$_6$] to fourfold coordination [WO$_4$] [28]. However, a more detailed study will be needed to confirm this change. The scattering extending from 550 to 870 cm^{-1} is mainly due to the overlap of two strong bands:

Table 1

Nominal composition (mol%), density (ρ), and molar volume (V_m) of the Nd^{3+}-doped TW glasses in Amb and O_2 atmospheres.

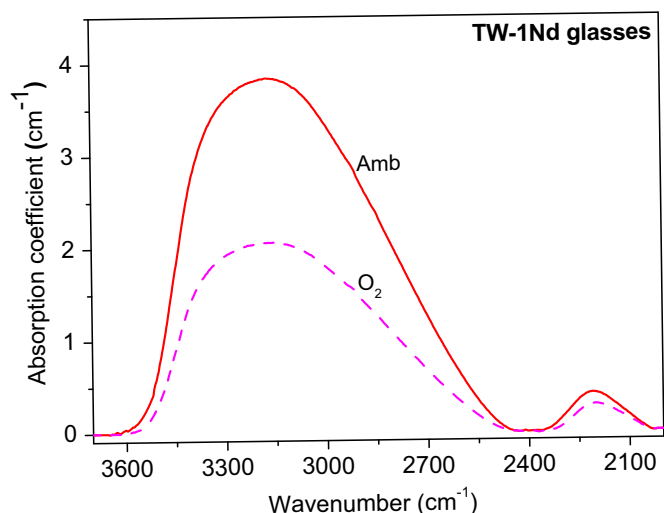| Sample	TeO$_2$ (mol%)	WO$_3$ (mol%)	Nd$_2$O$_3$ (mol%)	ρ (Amb)* (g/cm^3)	V_m (Amb) (cm^3/mol)	ρ (O$_2$)* (g/cm^3)	V_m (O$_2$) (cm^3/mol)
TW	80	20	0	5.89	29.55	5.88	29.60
TW-0.05Nd	79.96	19.99	0.05	5.89	29.56	5.88	29.61
TW-0.5Nd	79.6	19.9	0.5	5.89	29.69	5.89	29.69
TW-1Nd	79.2	19.8	1.0	5.89	29.83	5.89	29.83
TW-2Nd	78.4	19.6	2.0	5.93	29.90	5.92	29.95
TW-4Nd	76.8	19.2	4.0	5.94	30.39	5.93	30.45

* The density error is 0.02.

Fig. 1. IR absorption spectra of the TW-1Nd glasses prepared in Amb and O_2 atmospheres.
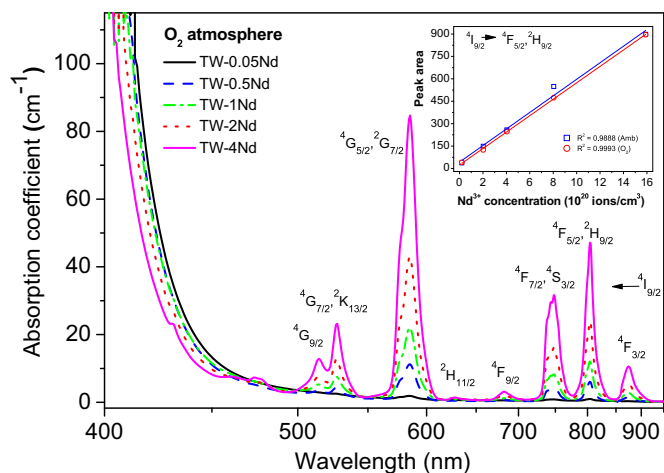

Fig. 2. VIS-NIR absorption spectra of the Nd^{3+}-doped TW samples prepared in an O_2 atmosphere. The inset shows the linear dependence of the $^4F_{5/2}$, $^2H_{9/2}$ absorption area with Nd^{3+} ions concentration. (For interpretation of the references to color in this figure legend, the reader is referred to the web version of this article.)
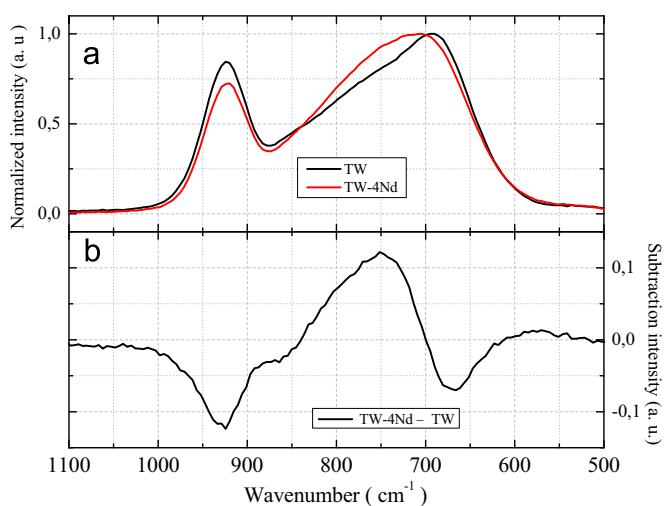

Fig. 3. (a) Raman absorption spectra of TW and TW-4Nd samples prepared in an O_2 atmosphere and (b) the difference between the two spectra ($I_{TW-4Nd} - I_{TW}$).

stretching vibrations of TeO_4 units (~ 670 cm^{-1}) and stretching vibrations of TeO_{3+1} or TeO_3 units (~ 750 cm^{-1}) [24,29,30]. In $80TeO_2$–$20WO_3$ glasses these two bands are not well defined as observed in other TW composition [29], unlike observed in the Raman spectra of the Nd^{3+}-doped TeO_2–ZnO–Nb_2O_5 (TZN) glass [24]. The addition of neodymium in TZN glass caused an inversion in the intensities of the peaks 670 and 750 cm^{-1} and they are almost the same for TZN with 5 mol% of neodymium. In order to evidence the difference among our samples, the Raman spectrum for TW-4Nd was subtracted from TW spectrum (showed in Fig. 3b). The intensity at 650 cm^{-1}, which is associated with Te–O bonds of TeO_4 units, decreases compared with that associated with Te–O bonds of $TeO_{3+1,3}$ units located at 750 cm^{-1}. So, the absorption edge shift to low wavelength observed in our glasses occurred due to structural changes (from tbp to tp).

The Nd absorption bands (centered at $\bar{\lambda}_{abs}$) in Fig. 2 were integrated to determine the area for JO calculation. In this model, parameters proportional to the oscillator strengths are measured (S_m) and calculated (S_c) for each absorption band (listed in Table. 2) [31]. In order to determine the Ω_2, Ω_4 and Ω_6 parameters, once Nd^{3+} transitions are assumed to be pure electric dipole, S_m and S_c are equal. All the obtained values are also exhibit in Table. 2. The Ω's obtained values are in good agreement to those reported in Ref. [4]. Furthermore, it was not observed any difference in the Ω's values among the group of studied samples (Amb and O_2). As usually done, the Ω's parameters can be applied to calculate the line strengths corresponding to the transitions from $^4F_{3/2} \rightarrow ^4I_{9/2}$, $^4I_{11/2}$, $^4I_{13/2}$ and $^4I_{15/2}$ of the Nd^{3+} ion, and with this, the radiative transition rates between two given levels $A_{JJ'}$ were calculated, and consequently the radiative lifetime ($\tau_{rad} \sim 154$ μs).

The emission spectra of the Nd^{3+}-doped glasses prepared in an O_2 atmosphere are presented in Fig. 4. The 514.5 nm radiation excites the Nd^{3+} ions to $^4G_{9/2}$ level, and after fast non-radiative decays, these excited ions reach the $^4F_{3/2}$ metastable state. The observed emission transitions occur from $^4F_{3/2}$ emitting level to the following: $^4I_{9/2}$ (~ 907 nm), $^9I_{11/2}$ (1065 nm), and $^9I_{13/2}$ (1337 nm). The inset of Fig. 4 shows that the intensity of emission transition at 1065 nm decreases as the Nd^{3+} concentration is increased. This decrease indicates that the total decay rate (W) increased due to the non-radiative decay rate (W_{NR}) meaning that the fraction of absorbed energy converted into heat (φ) increased.

Fig. 5 shows the fluorescence decay curves for $^4F_{3/2} \rightarrow ^4I_{11/2}$ transition of the Nd^{3+}-doped TW samples prepared under O_2 atmosphere, and similar curves were also obtained for the samples prepared in Amb atmosphere. The measured lifetime (τ_{exp}) of $^4F_{3/2}$ level for each doped sample was determined fitting the experimental fluorescence decay curve with a single exponential dependence (Table. 3). The total decay rate for $^4F_{3/2}$ (Nd^{3+}) level was evaluated by the reciprocal of the measured lifetime, which is given by $W = \tau_{exp}^{-1} = W_R + W_{NR}$, where W_R is the sum of all radiative decay rates originating from the $^4F_{3/2}$ level. The obtained values are also presented in Table. 3. $W_R = 1/\tau_{rad}$ was obtained by the JOΩ's parameters and, as a consequence, the W_{NR} can be evaluated as follows:
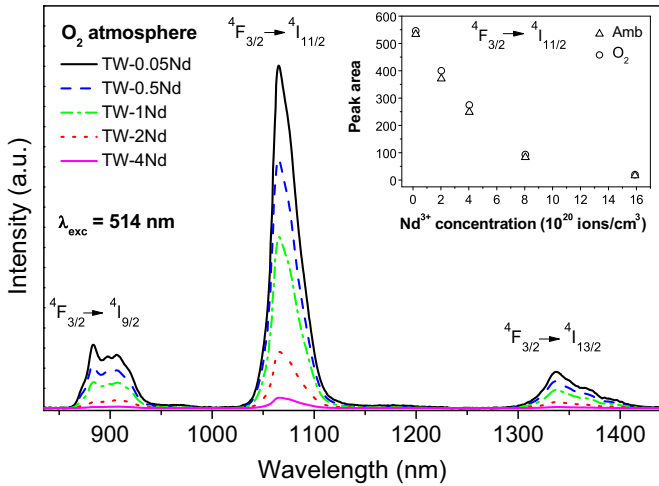
$$W_{NR} = \frac{1}{\tau_{exp}} - \frac{1}{\tau_{rad}} \tag{1}$$

For the lowest Nd^{3+} concentration sample, the measured and the calculated radiative lifetime values are similar, for both atmosphere, indicating a very small energy loss by nonradiative process. They also are in agreement to those reported in other studies using Nd^{3+}-doped tungsten–tellurite glasses [4]. As can be seen, W_{NR} increases greatly with the increase of the Nd^{3+} concentration, which is the sum of the following non-radiative processes: cross-relaxation between Nd^{3+} ions (W_{CR}) ($^4F_{3/2} \rightarrow ^4I_{5/2}$:

Table 2

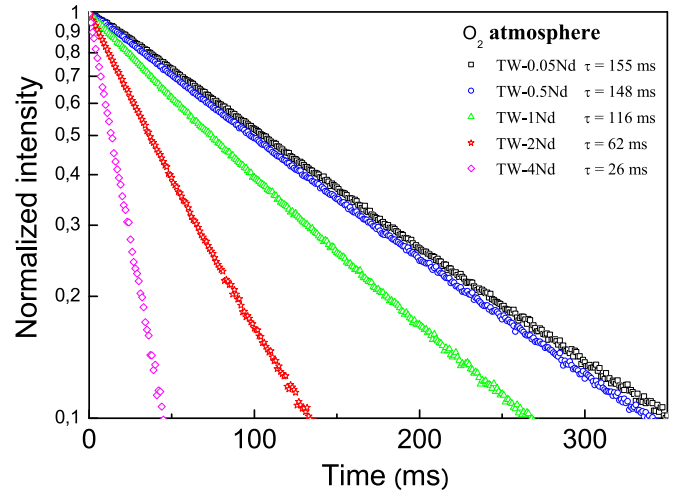Absorption and emission parameters and JO intensity parameters of TW-1Nd glasses prepared in O_2 atmosphere. The Ω´s values obtained for the other samples are similar, including those prepared in Amb atmosphere.

$\bar{\lambda_{abs}}$ (nm)	S_m ($\times 10^{-20}$ cm^2)	S_c ($\times 10^{-20}$ cm^2)	$|S_m - S_c|$ ($\times 10^{-20}$ cm^2)
526			
	1.6	1.5	0.1
585			
	6.56	6.57	0.01
682			
	0.16	0.17	0.01
748			
	2.39	2.46	0.07
804			
	2.73	2.65	0.08
874			
	0.8	1.0	0.2

Ω_2 ($\times 10^{-20}$ cm^2)	Ω_4 ($\times 10^{-20}$ cm^2)	Ω_6 ($\times 10^{-20}$ cm^2)
4.6		
	3.3	3.5
RMS $= 4.6 \times 10^{-21}$		

Transition from $^4F_{3/2}$ to	$\bar{\lambda}$ (nm)	$A_{JJ'}$ (s^{-1})	τ_{rad} (µs)
$^4I_{15/2}$			154 $\pm$ 4
	1900	30.3	
$^4I_{13/2}$			
	1337	669.9	
$^4I_{11/2}$			
	1065	3138.4	
$^4I_{9/2}$			
	907	2695.3	

Fig. 4. Emission spectra of Nd^{3+}-doped TW glasses in the O_2 atmosphere. The inset shows the intensity behavior of the $^4F_{3/2} \rightarrow {}^4I_{11/2}$ transition.

Fig. 5. Luminescence decay from $^4F_{3/2}$ level of the Nd^{3+}-doped TW glasses prepared under O_2 atmosphere.

$^4I_{9/2} \rightarrow {}^4I_{15/2}$), energy transfer rate from Nd^{3+} to OH$^-$ ions (W_{OH}), and multiphonon relaxation rate (W_{MP}). The latter rate depends on the temperature, the energy gap between the $^4F_{3/2}$ and $^4I_{15/2}$ levels, and the phonon energy of the host glass [32,33]. In a room temperature environment, W_{MP} is very low ($\sim 2 \times 10^{-3}$ s^{-1}) for all present Nd^{3+}-doped tellurite glasses independent of the environmental conditions in which they have been prepared. Therefore, it can be disregarded. Furthermore, W_{MP} is the same for all samples because the maximum phonon energy is practically independent (around 940 cm^{-1}) with the increase of Nd^{3+} concentration.

W_{OH} is proportional to the donor (Nd^{3+}) and acceptor (OH$^-$) concentrations and the absorption coefficient of the OH$^-$ free (α_{OH}), which can be defined as follows [19,33,34]:

$$W_{OH} = K_{Nd-OH} \, N_{Nd} \, \alpha_{OH} \tag{2}$$

where K_{Nd-OH} is a constant determined by the force of interactions between Nd^{3+} and OH$^-$ ions and is independent of the concentration of these ions. The value of this constant for interaction between Er^{3+} and OH$^-$ ions is practically the same in tetraphosphate (15×10^{-19} cm^4 s^{-1}) [19] and tellurite (14×10^{-19} cm^4 s^{-1}) [33] glasses. Thus, taking the K_{Nd-OH} value equal to that

Table 3
Experimental lifetime (τ_{exp}), reciprocal of the experimental lifetimes (W), non-radiative rate (W_{NR}), energy transfer rate between Nd^{3+} and OH^{-} ions (W_{OH}), and cross-relaxation rate (W_{CR}) for Nd^{3+}-doped TW glasses prepared in the Amb and O_2 atmospheres.

Sample	τ_{exp} (µs)		$W = 1/\tau_{exp}$ (10^3 s^{-1})		$W_{NR} = \tau_{exp}^{-1}\tau_{rad}^{-1}$($10^3$ s^{-1})		W_{OH} (10^3 s^{-1})		$W_{CR} = W_{NR} - W_{HO}$ (10^3 s^{-1})	
	Amb	O_2	Amb	O_2	Amb	O_2	Amb	O_2	Amb	O_2
TW-0.05Nd	152 ± 1	155 ± 1	6.58 ± 0.04	6.45 ± 0.04	–	–	–	–	–	–
TW-0.5Nd	141 ± 1	148 ± 1	7.09 ± 0.05	6.76 ± 0.05	0.6 ± 0.2	0.3 ± 0.2	0.6 ± 0.1	0.4 ± 0.1	–	–
TW-1Nd	115 ± 1	116 ± 1	8.70 ± 0.08	8.62 ± 0.08	2.2 ± 0.3	2.2 ± 0.3	1.0 ± 0.1	0.5 ± 0.1	1.2 ± 0.4	1.7 ± 0.4
TW-2Nd	58 ± 1	62 ± 1	17.2 ± 0.3	16.1 ± 0.3	10.7 ± 0.5	9.7 ± 0.5	1.6 ± 0.2	0.7 ± 0.1	9.1 ± 0.7	9.0 ± 0.6
TW-4Nd	22 ± 1	26 ± 1	45 ± 2	38 ± 1	39 ± 2	32 ± 1	2.9 ± 0.2	1.6 ± 0.2	36 ± 2	30 ± 1

obtained in tetraphosphate glasses (6.2×10^{-19} cm^4 s^{-1}), it was possible to estimate the value of W_{OH} for each sample and, consequently, the value of W_{CR}. Although α_{OH} decreases with increasing Nd^{3+} concentration, the product of N_{Nd} and α_{OH} increased and, consequently, W_{OH} is also increased. It is interesting to note that the W_{OH} values for the Nd^{3+}-doped samples prepared in O_2 atmosphere are lower than the values for the samples prepared in Amb.

The subtracting among W_{NR} and W_{OH}, W_{CR} was calculated and the values are also listed in Table 3. Unlike W_{OH}, W_{CR} values increase greatly with the Nd^{3+} concentration mainly because of W_{NR} values (W_{OH} contributes to W_{CR} with less than 10%). Futhermore, for TW-4Nd sample prepared in O_2 atmosphere the W_{CR} value is approximately 20% lower than those prepared in Amb. It was not possible to note difference among W_{NR} and W_{OH} for samples prepared with lowest Nd^{3+} concentration, indicating that both equally contribute to W_{CR}.

The findings discussed so far suggest that when Nd^{3+} ions were added in the sample, the luminescence quantum efficiency (η) of the $^4F_{3/2}$ level decreased (due to the noted increment in W_{NR}). As a consequence, the fraction of energy absorbed by the sample and converted into heat (φ) should increase. η can be evaluated using the radiative and experimental lifetimes ($\eta = \tau_{exp}/\tau_{rad}$). In the context of our work, this term will be referenced as luminescence quantum efficiency from JO (η_{JO}). On the other hand, the TL technique allows us to evaluate η as well as φ, which can be determined using this equation [20–21]:

$$\phi C = -\frac{\theta}{\alpha\, L_{eff}\, P_e} = \Theta \tag{3}$$

where θ is the TL signal amplitude obtained by fitting the experimental curves, α is the absorption coefficient, $L_{eff} = (1 - e^{-\alpha L})/\alpha$ is the effective thickness of the sample, L is the thickness, P_e is the excitation power, and $C = (ds/dT)/K\lambda_p$ is the intrinsic parameters for the matrix. In this parameter, K is the thermal conductivity, ds/dT is the temperature coefficient of the optical path length, and λ_p is the probe beam wavelength.

As the undoped samples present no fluorescence, $\varphi = 1$ and in this case C is equal to Θ, whose measured value ($\Theta = 37$ W^{-1}) is close to that obtained for TLT glasses (34 W^{-1}) [35]. Therefore, the value of φ for the doped samples was determined by comparing the data of doped samples (Θ_d) with those of the undoped ones (Θ_{und}) ($\phi = \Theta_d/\Theta_{und}$), as is usually done in the η determination by TL technique [21]. When the Nd^{3+} concentration increased from 0.5 to 4 mol%, the fraction of absorption energy converted in heat increased from 0.39 to 0.95 and from 0.41 to 0.88, respectively, for samples prepared in Amb and O_2 atmospheres.

Having the φ values, it was possible to evaluate η using the relationship [21]:

$$\phi = 1 - \eta\frac{\langle\nu_{em}\rangle}{\nu_{ex}} \tag{4}$$

where ν_{ex} and $\langle\nu_{em}\rangle$ are the excitation and the average emission
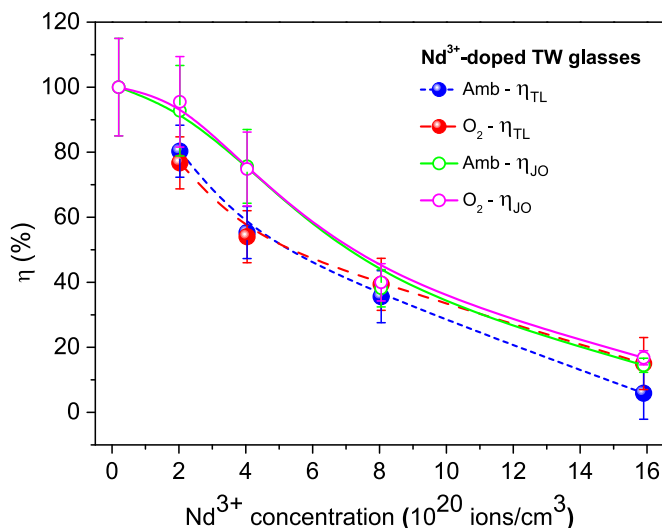
Fig. 6. Luminescence quantum efficiency calculated by the Judd–Ofelt theory and measured by TL technique for the Nd^{3+}-doped TW glasses in the Amb and O_2 atmospheres.

wavenumber, respectively. For our studied Nd^{3+}-doped samples, $\langle\nu_{em}\rangle = 9381$ cm^{-1} and for our experimental setup, $\nu_{ex} = 12{,}318$ cm^{-1}. Fig. 6 shows a comparison between luminescence quantum efficiencies obtained by the JO method (η_{JO}) and by the TL technique (η_{TL}) for both of the sample sets. The observed difference between the η values is within the margin of error of both of the methods used. The same behavior was observed in other works: Suzuki et al. [36] observed that the quantum efficiency of the Nd^{3+}-doped TeO_2–K_2O glass varied from 86% at 0.05 mol% of Nd_2O_3 to 18% at 2 mol% and concluded that this decrease was due to concentration quenching. Jaba et al. [37] concluded that the decrease from 166 µs at 0.2 mol% to 62 µs at 62% was due solely to energy transfer between Nd^{3+} ions. Rajeswari et al. [38] concluded that the observed decrease in the fluorescence (from 93% to 33%) accompanied by an increase in the Nd_2O_3 concentration was due to cross-relaxation among Nd^{3+}–Nd^{3+} ions. They found the multiphonon relaxation rate from $^4F_{3/2}$ level to be negligible.

4. Conclusion

TW glasses doped with various concentrations of Nd^{3+} ions were prepared in air and O_2-rich atmospheres in order to obtain glasses with better spectroscopic properties. Measurements of the optical absorption, luminescence, and lifetime were performed. From the TL data, it was possible to determine the heat absorbed by the glass samples and consequently, the luminescence quantum efficiency. We can conclude from this investigation that: (1) in each sample set, the increase of Nd^{3+} ions into the $80TeO_2$–$20WO_3$

matrix caused structural changes (TeO$_4$→TeO$_3$) causing a blue-shift of the absorption edge; (2) the cross-relaxation was the main loss mechanism in fluorescence for Nd^{3+} ions concentrations greater than 1%; (3) the quantum efficiencies evaluated by JO and TL are in agreement, and the small observed differences are within their margin of error; (4) the luminescence quantum efficiency for lowest concentration of Nd^{3+} is close to unity; and (5) the OH$^-$ ions reduction into the Nd^{3+}-doped TW glass slightly increase the ^{4}F$_{3/2}$ level lifetime value, but the improvement in the luminescence quantum efficiency was not determined by TL measurements because it is within the experimental error. Important to mention that, although it was observed a reduction in W$_{OH}$ from Amb to O$_2$ synthesis procedure, all the calculated values for W_{OH} are lower than the W_{NR} values, mainly for higher Nd^{3+} concentration. This suggests that W_{NR} is dominant in heating the sample, so that some improvement in the optical quality sample due W_{OH} is difficult to be measured by TL technique.

Acknowledgments

References

[1] J.S. Wang, D.P. Machewirth, F. Wu, E. Snitzer, Neodymium-doped tellurite single-mode fiber laser, Opt. Lett. 19 (1994) 1448–1449.
[2] N. Lei, B. Xu, Z. Jiang, Ti:sapphire laser pumped Nd: tellurite glass laser, Opt. Commun. 127 (1996) 263–265.
[3] I. Iparraguirre, J. Azkargorta, J.M. Fernández-Navarro, M. Al-Saleh, J. Fernández, R. Balda, Laser action and upconversion of Nd^{3+} in tellurite bulk glass, J. Non-Cryst. Solids 353 (2007) 990–992.
[4] H. Kalaycioglu, H. Cankaya, G. Ozen, L. Ovecoglu, A. Sennaroglu, Lasing at 1065 nm in bulk Nd^{3+}-doped telluride-tungstate glass, Opt. Commun. 281 (2008) 6056–6060.
[5] H. Cankaya, A. Sennaroglu, Bulk Nd^{3+}-doped tellurite glass laser at 1.37 μm, Appl. Phys. B 99 (2010) 121–125.
[6] D.F. De Sousa, L.A.O. Nunes, J.H. Rohling, M.L. Baesso, ML, Laser emission at 1077 nm in Nd^{3+}-doped calcium aluminosilicate glass, Appl. Phys. B 77 (2003) 59–63.
[7] J.C. Michel, D. Morin, F. Auzel, Propriétés spectroscopiques et effet laser d'un verre tellurite et d'un verre phosphate fortement dopés en néodyme, Rev. Phys. Appl. 13 (1978) 859–866.
[8] A. Jha, B. Richards, G. Jose, T. Teddy-Fernandez, P. Joshi, X. Jiang, J. Lousteau, Rare-earth ion doped TeO$_2$ and GeO$_2$ glasses as laser materials, Prog. Mater. Sci. 57 (2012) 1426–1491.
[9] J.S. Wang, E.M. Vogel, E. Snitzer, Tellurite glass: a new candidate for fiber devices, Opt. Mater. 3 (1994) 187–203.
[10] G.N. Conti, S. Berneschi, M. Bettinelli, M. Brenci, B. Chen, S. Pelli, A. Speghini, G. C. Righini, Rare-earth doped tungsten tellurite glasses and waveguides: fabrication and characterization, J. Non-Cryst. Solids 345–346 (2004) 343–348.
[11] S. Sakida, T. Nanba, Y. Miura, Optical properties of Er^{3+}-doped tungsten tellurite glass waveguides by Ag$^+$–Na$^+$ ion exchange, Opt. Mater. 30 (2007) 586–593.
[12] P.W. Kuan, K. Li, G. Zhang, X. Wang, L. Zhang, G. Bai, Y. Tsang, L. Hu, Compact broadband amplified spontaneous emission in Tm^{3+}-doped tungsten tellurite glass double-cladding single-mode fiber, Opt. Mater. Express 3 (2013) 723–728.
[13] K. Li, G. Zhang, X. Wang, L. Hu, P. Kuan, D. Chen, M. Wang, Tm^{3+} and Tm^{3+}–Ho^{3+} co-doped tungsten tellurite glass single mode fiber laser, Opt.

Express 20 (2012) 10115–10121.
[14] K. Li, G. Zhang, L. Hu, Watt-level ~2 μm laser output in Tm^{3+}-doped tungsten tellurite glass double-cladding fiber, Opt. Lett. 35 (2010) 4136–4138.
[15] C. Lasbrugnas, P. Thomas, O. Masson, J.C. Champarnaud-Mesjard, E. Fargin, V. Rodriguez, M. Lahaye, Second harmonic generation of thermally poled tungsten tellurite glass, Opt. Mater. 31 (2009) 775–780.
[16] H. Ebendorff-Heidepriem, K. Kuan, M.R. Oermann, K. Knight, T.M. Monro, Extruded tellurite glass and fibers with low OH content for mid-infrared applications, Opt. Mater. Express 2 (2012) 432–442.
[17] P.E. Wang, W.N. Li, B. Peng, M. Lu, Effect of dehydration techniques on the fluorescence spectral features and OH absorption of heavy metals containing fluoride tellurite glasses, J. Non-Cryst. Solids 358 (2012) 788–793.
[18] G. Navarra, I. Iliopoulos, V. Militello, S.G. Rotolo, M. Leone, OH-related infrared absorption bands in oxide glasses, J. Non-Cryst. Solids 351 (2005) 1796–1800.
[19] L. Zhang, H. Hu, The effect of OH$^-$ on IR emission of Nd^{3+}, Yb^{3+} and Er^{3+} doped tetraphosphate glasses, J. Phys. Chem. Solids 63 (2002) 575–579.
[20] J. Shen, R.D. Lowe, R.D. Snook, A model for cw laser induced mode-mismatched dual-beam thermal lens spectrometry, Chem. Phys. 165 (1992) 385–396.
[21] S.M. Lima, J.A. Sampaio, T. Catunda, A.C. Bento, L.C.M. Miranda, M.L. Baesso, Mode-mismatched thermal lens spectrometry for thermo-optical properties measurement in optical glasses: a review, J. Non-Cryst. Solids 273 (2000) 215–227.
[22] A.M. Efimov, T.G. Kostyreva, G.A. Sycheva, Water-related IR absorption spectra for alkali zinc pyrophosphate glasses, J. Non-Cryst. Solids 238 (1998) 124–142.
[23] M.D. O'Donnell, C.A. Miller, D. Furniss, V.K. Tikhomirov, A.B. Seddon, Fluorotellurite glasses with improved mid-infrared transmission, J. Non-Cryst. Solids 331 (2003) 48–57.
[24] V. Kamalaker, G. Upender, C.H. Ramesh, V.C. Mouli, Raman spectroscopy, thermal and optical properties of TeO$_2$–ZnO–Nb$_2$O$_5$–Nd$_2$O$_3$ glasses, Spectrochim. Acta A 89 (2012) 149–154.
[25] V. Nazabal, S. Todoroki, A. Nukui, T. Matsumoto, S. Suehara, T. Hondo, T. Araki, S. Inoue, C. Rivero, T. Cardinal, Oxyfluoride tellurite glasses doped by erbium: thermal analysis, structural organization and spectral properties, J. Non-Cryst. Solids 325 (2003) 85–102.
[26] G. Liao, Q. Chen, J. Xing, H. Gebavi, D. Milanese, M. Fokine, M. Ferraris, Preparation and characterization of new fluorotellurite glasses for photonics application, J. Non-Cryst. Solids 355 (2009) 447–452.
[27] Y. Gandhi, I.V. Kityk, M.G. Brik, P. Raghava Rao, N. Veeraiah, Influence of tungsten on the emission features of Nd^{3+}, Sm^{3+} and Eu^{3+} ions in ZnF$_2$–WO$_3$–TeO$_2$ glasses, J. Alloy. Compd. 508 (2010) 278–291.
[28] A.E. Ersundu, M. Çelikbilek, N. Solak, S. Aydin, Glass formation area and characterization studies in the CdO-WO$_3$–TeO$_2$ ternary system, J. Eur. Ceram. Soc. 31 (2011) 2775–2781.
[29] G. Upender, S. Bharadwaj, A.M. Awasthi, V.C. Mouli, Glass transition temperature-structural studies of tungstate tellurite glasses, Mater. Chem. Phys. 118 (2009) 298–302.
[30] V.O. Sokolov, V.G. Plotnichenko, E.M. Dianov, Structure of WO$_3$–TeO$_2$ glasses, Inorg. Mater. 43 (2007) 194–212.
[31] S.M. Limna, J.A. Sampaio, T. Catunda, A.S.S. de Camargo, L.A.O. Nunes, M. L. Baesso, D.W. Hewak, Spectroscopy, thermal and optical properties of Nd^3 +-doped chalcogenide glasses, J. Non-Cryst. Solids 284 (2001) 274–281.
[32] J.M.F. van Dijk, M.F.H. Schuurmans, On the nonradiative and radiative decay rates and a modified exponential energy gap law for 4f–4f transitions in rare-earth ions, J. Chem. Phys. 78 (1983) 5317–5323.
[33] Y. Guo, M. Li, L. Hu, J. Zhang, Effect of fluorine ions on 2.7 μm emission in Er^{3+}/Nd^{3+}-codoped fluorotellurite glass, J. Phys. Chem. A 116 (2012) 5571–5576.
[34] H. Ebendorff-Heidepriem, W. Seeber, D. Ehrt, Spectroscopic properties of Nd^{3+} ions in phosphate glasses, J. Non-Cryst. Solids 183 (1995) 191–200.
[35] S.M. Lima, W.F. Falco, E.S. Bannwart, L.H.C. Andrade, R.C. Oliveira, J.C.S. Moraes, K. Yukimitu, E.B. Araújo, E.A. Falcão, A. Steimacher, N.G.C. Astrath, A.C. Bento, A.N. Medina, M.L. Baesso, Thermo-optical characterization of tellurite glasses by thermal lens, thermal relaxation calorimetry and interferometric methods, J. Non-Cryst. Solids 352 (2006) 3603–3607.
[36] T. Suzuki, H. Kawai, H. Nasu, M. Hughes, Y. Ohishi, S. Mizuno, H. Ito, K. Hasegawa, Quantum efficiency of Nd^{3+}-doped glasses under sunlight excitation, Opt. Mater. 33 (2011) 1952–1957.
[37] N. Jaba, A. Kanoun, H. Mejri, A. Brenier, Time-resolved luminescence data on the 1060 nm transition in Nd^{3+}-doped zinc tellurite glasses, J. Phys.: Condens. Matter 12 (2000) 7303–7309.
[38] R. Rajeswari, S.S. Babu, C.K. Jayasankar, Spectroscopic characterization of alkali modified zinc-tellurite glasses doped with neodymium, Spectrochim. Acta A 77 (2010) 135–140.